

Interfacial reactions between Sn-2.5Ag-2.0Ni solder and electroless Ni(P) deposited on SiC_p/Al composites

WU Mao(吴 茂), QU Xuan-hui(曲选辉), HE Xin-bo(何新波), Rafi-ud-din,
REN Shu-bin(任淑彬), QIN Ming-li(秦明礼)

State Key Laboratory for Advanced Metals and Materials, School of Materials Science and Engineering,
University of Science and Technology Beijing, Beijing 100083, China

Received 9 June 2009; accepted 14 September 2009

Abstract: A novel Sn-2.5Ag-2.0Ni alloy was used for soldering SiC_p/Al composites substrate deposited with electroless Ni(5%P) (mass fraction) and Ni(10%P) (mass fraction) layers. It is observed that variation of P contents in the electroless Ni(P) layer results in different types of microstructures of SnAgNi/Ni(P) solder joint. The morphology of Ni₃Sn₄ intermetallic compounds (IMCs) formed between the solder and Ni(10%P) layer is observed to be needle-like and this shape provides high speed diffusion channels for Ni to diffuse into solder that culminates in high growth rate of Ni₃Sn₄. The diffusion of Ni into solder furthermore results in the formation of Kirkendall voids at the interface of Ni(P) layer and SiC_p/Al composites substrate. It is observed that solder reliability is degraded by the formation of Ni₂SnP, P rich Ni layer and Kirkendall voids. The compact Ni₃Sn₄ IMC layer in Ni(5%P) solder joint prevents Ni element from diffusing into solder, resulting in a low growth rate of Ni₃Sn₄ layer. Meanwhile, the formation of Ni₂SnP that significantly affects the reliability of solder joints is suppressed by the low P content Ni(5%P) layer. Thus, shear strength of Ni(5%P) solder joint is concluded to be higher than that of Ni(10%P) solder joint. Growth of Ni₃Sn₄ IMC layer and formation of crack are accounted to be the major sources of the failure of Ni(5%P) solder joint.

Key words: SnAgNi solder; electroless Ni(P); SiC_p/Al composites; intermetallic compound; interfacial reaction

1 Introduction

SiC_p/Al metal matrix composite possesses a combination of novel properties, including a thermal expansion coefficient which is compatible to an electronic device or substrate, high thermal conductivity, low density as well as high mechanical strength. Such a combination of properties makes the composite a valuable packaging material for electronic applications. Main application fields of the material are heat sinks, substrates, enclosures and base plates of various power modules, where the requirement for thermal management is high and the limitation imposed to weight of the material is stringent[1]. Most of the research about SiC_p/Al composite revolves its production techniques, but less was carried out on its post-processing techniques such as welding and heat treatment[1–8].

SiC_p/Al composite can replace Kovar alloy and it is

used in making seals and carriers of ceramic package for discrete transistors, diodes and integrated circuits. These package forms offer accurate component placement, attachment, sealing, protection and various electrical, optical and fluidic interconnects. These assemblies usually have longer shelf-lives and require hermetic sealing. Package sealing can be obtained by using a variety of materials including epoxies and solders[9]. Among them, Sn2.5Ag2.0Ni solder is well suited for soldering optoelectronic devices and hermetic sealing applications. In this study, Sn2.5Ag2.0Ni is used to join SiC_p/Al composites lids and enclosures.

Ni is well-recognized as a good diffusion barrier between substrate and solder due to its negligible solubility in Sn-based solder as well as low growth rate of Sn-Ni intermetallics[10–15]. Therefore, conventional surface finishing metallization on the Kovar alloy substrate is a Ni/Au deposition by electroplating. However, it is difficult to deposit Ni layer on the SiC_p/Al

composites by electroplating due to the existence of the nonmetallic SiC particles. Therefore, an electroless Ni plating process is employed for the metallization of SiC_p/Al composites. But, conventional available plating solutions of electroless Ni in industry usually contain relatively high contents (9%–10%, mass fraction) of P, which would reduce the solder joint reliability[10]. In order to reduce the phosphorus content, another type of Ni(P) solution with a low P-content (5%, mass fraction) was considered. The effects of P contents of Ni plating on microstructure evolution and reliability of solder joint were not yet available in the literature and they are investigated in the present work.

The present study aims at assessing the reliability of Sn_{2.5}Ag_{2.0}Ni solder attachment of the SiC_p/Al composite substrates with various Ni coatings. The electroless Ni layers under evaluation are Ni(5%P) and Ni(10%P). The reliability of solder joint was measured by mechanical shear tests. Furthermore, the effects of thermal aging on microstructure evolution were also investigated. Failure modes related to solder joint were evaluated and a possible mechanism was proposed.

2 Experimental

A directly palladium activation step was employed to succeed in electroless Ni plating on SiC_p/Al composites. Prior to being plated, the composites surfaces were degreased in an alkaline solution containing 20 g/L Na₃PO₄, 5 g/L NaOH and 10 g/L Na₂CO₃ at 65 °C for 2 min, and then immersed in an acidic solution containing 10% HNO₃ and 10% HF at 25 °C for 1 min. SiC_p/Al composites were then sensitized in a SnCl₂ solution containing 10 g/L SnCl₂ and 200 mL/L HCl at 25 °C for 1 min, and then activated in a PdCl₂ acidic solution containing 0.25 g/L PdCl₂ and 10 mL/L HCl at 25 °C for 2 min. The electroless Ni(P) plating was deposited using a bath containing sulfate (NiSO₄·7H₂O) as the source of nickel and sodium hypophosphite (NaH₂PO₂·H₂O) as the reductant. Table 1 lists the chemical composition of electroless Ni(P) layer. The P content in Ni(P) layer is 10% (mass fraction) from acidic bath and 5% (mass fraction) from alkaline bath, respectively. The mean initial thickness of these electroless Ni coatings is about 4–6 μm. During the electroless process, the pH values of all solutions were adjusted by diluted NaOH or H₂SO₄ and controlled by a PHS-25 pH controller.

The Sn_{2.5}Ag_{2.0}Ni solder was in plate-like shape with a thickness of 100 μm. Soldering process was conducted in a tubular furnace under nitrogen (N₂) atmosphere, and conventional rosin moderate activated (RMA) flux was used. The soldering temperature was 280 °C and holding time was 4 min. The heating and

Table 1 Chemical composition of electroless Ni(P) plating

Chemical composition	Concentration in acid bath (pH=6.5, 65 °C)	Concentration in alkaline bath (pH=8.5, 45 °C)
NiSO ₄ ·7H ₂ O	30 g/L	20 g/L
NaH ₂ PO ₂ ·H ₂ O	30 g/L	30 g/L
Na ₃ C ₆ H ₅ O ₇ ·2H ₂ O	30 g/L	10 g/L
(NH ₄) ₂ SO ₄	20 g/L	–
NH ₄ Cl	–	30 g/L
C ₂ H ₅ OCOOH	15 mL/L	10 mL/L

cooling rates were set at 20 °C/min, and one specimen was prepared each time. Soldering process is followed by isothermal aging solder joints in an oven at 150 °C for 0, 50, 250, 500, and 1 000 h, respectively.

The morphology and fracture surface of solder joints were observed by LEO1450 scanning electron microscopy (SEM) and energy dispersive X-ray spectroscopy (EDX). The mean thickness of Ni(P) layer was measured on SEM micrographs, and the P content at half thickness of the Ni(P) layer was tested by EDX. The shear test was performed at room temperature with a RG3000A micro-tester at a speed of 0.2 mm/min. To obtain reliable results, 10 specimens were prepared for each experimental condition, so the final results were the average values in 10 experiments. Fracture surface and cross-section perpendicular to solder joint were also characterized by optical microscopy and SEM.

3 Results and discussion

3.1 Effect of P content on microstructure

The differential scanning calorimetry (DSC) curve of Sn_{2.5}Ag_{2.0}Ni solder was taken at a heating rate of 10 °C/min, as shown in Fig.1. The highest temperature of the endothermic peak is about 237.3 °C. Therefore, the soldering process is carried out at a temperature of 280 °C for 4 min.

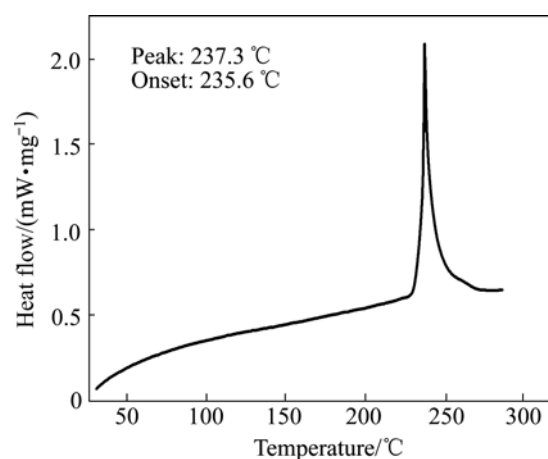


Fig.1 DSC curve of Sn-Ag-Ni solder

Fig.2 depicts the variation in the morphology of the SnAgNi/Ni(P) solder joint with P contents of 10% and 5% (mass fraction) in Ni(P) coatings. During the soldering process, the Ni in Ni(P) layer reacts with solder, and relatively fast diffusion of nickel at certain locations results in the different shapes and thicknesses of Ni_3Sn_4 IMC grains along the interface, and a P-rich Ni layer at the SnAgNi/Ni(10%P) interface. It is expected that the diffusion of Ni into the solder makes Ni deplete inside the Ni(P) layer and results in a corresponding accumulation of P in the remaining Ni(P). Apart from the P-rich Ni layer, a very thin Sn-Ni-P layer is formed at the interface between the P-rich Ni layer and solder (Fig.2(a)). EDX results show that molar ratio of the Ni-Sn-P layer is Sn:Ni:P=22.1:52.4:25.5. According to the studies by LIN et al[16], LIN and DUH[17] and KANG et al[18], the Ni-Sn-P layer corresponds to the ternary Ni_2SnP phase. However, most studies reported that joint reliability was degraded by formation of additional layers, such as ternary Ni-Sn-P and P-rich Ni layers. The formation of the ternary Ni-Sn-P phase seriously affects the reliability of the joint, since a rather thin ($<1 \mu\text{m}$) and flat Ni-Sn-P phase fails to play an interlocking role at the interface between solders and coatings. In contrast, a thick (about 2–3 μm) and wavy Ni-Sn IMC plays a mechanical interlocking role in the solder joint[17, 19]. The mechanical reliability is degraded when a P-rich Ni layer is formed because it cracks easily[20–21].

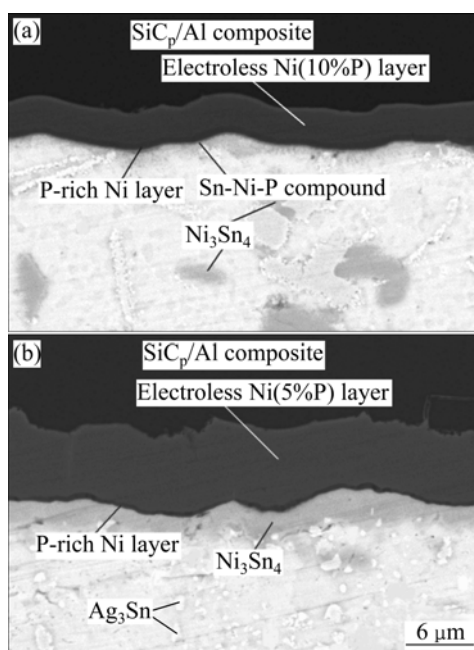


Fig.2 SEM images of SnAgNi/Ni(P) solder joints with different initial P contents in electroless Ni(P) layer: (a) 10%, (b) 5%

Fig.2(b) shows the microstructure of solder joint with 5% P in Ni(P) layer. Ni_3Sn_4 IMC and a dark P-rich

Ni layer are also observed at the solder joint. It is interesting to note that no Ni_2SnP phase is observed at the interface. Close examination of the cross-section reveals that the P-rich Ni layer is Ni_3P phase (74.3% Ni, 25.7% P, mole fraction). The Ni_3P forms as a result of Ni depletion inside the Ni(P) layer, which facilitates the crystallization of the amorphous Ni(P)[22]. According to LIU and SHANG [23], the Ni_3P phase is more stable in Ni-P system than Ni_{12}P_5 , which is an intermediate phase and easily transformed to other Ni-P phase. As long as Ni_{12}P_5 is converted into Ni_2P , the Ni-Sn-P phase will form due to Sn diffusion from the solder matrix[24–25]. Therefore, the formation of Ni_2SnP , which significantly affects the mechanical reliability of solder joints, is suppressed by the low P content Ni(5%P) layer in this study.

3.2 Aging behavior

Microstructures of solder joint with Ni(10%P) layer aged at 150 °C for various time are shown in Fig.3. No new IMCs form at the SnAgNi/Ni(P) interface during aging, but the thickness of Ni_3Sn_4 increases with the increase of aging time. It is found that the morphology of Ni_3Sn_4 IMC layer is more needle-like after aging for 500 h and the channels between these needle-shaped IMCs lead to higher diffusion rate of Ni and Sn, hence result in high growth rate of Ni_3Sn_4 IMC layer. The high diffusion rate can also be envisaged from the presence of a thin white layer (Sn-rich white layer) between Ni-Sn-P layer and IMCs after long term aging (Fig.3(c) and Fig.3(d)). This thin white layer (Sn-rich white layer) comes in contact with P-rich Ni layer through Ni_2SnP compound at the interface, resulting in a higher diffusion rate.

Fig.4 shows the microstructures of solder joint with Ni(5%P) layer aged at 150 °C for various time. It is interesting to note that the shape of Ni_3Sn_4 IMC layer is more compact in comparison with that in the case of Ni(10%P) solder joint. The compact Ni_3Sn_4 IMC layer leads to a relatively low diffusion rate of Ni and Sn. However, the compact Ni_3Sn_4 IMC layer also causes comparatively high thermal stress resulting from the difference in coefficient of thermal expansion between IMCs and solder.

The change in average thickness of Ni_3Sn_4 IMC layer with increasing aging time at 150 °C is shown in Fig.5. The IMC thickness increases linearly with the square root of the aging time at a fixed aging temperature. This indicates that the IMC growth in all of the systems under discussion is a diffusion-controlled process. The initial IMCs thickness of Ni(5%P) and Ni(10%P) solder joints are 1.5 and 1.7 μm , respectively. The growth rate of IMCs in SnAgNi/Ni system is proportional to $t^{1/2}$ at 150 °C as determined by linear regression analysis. The

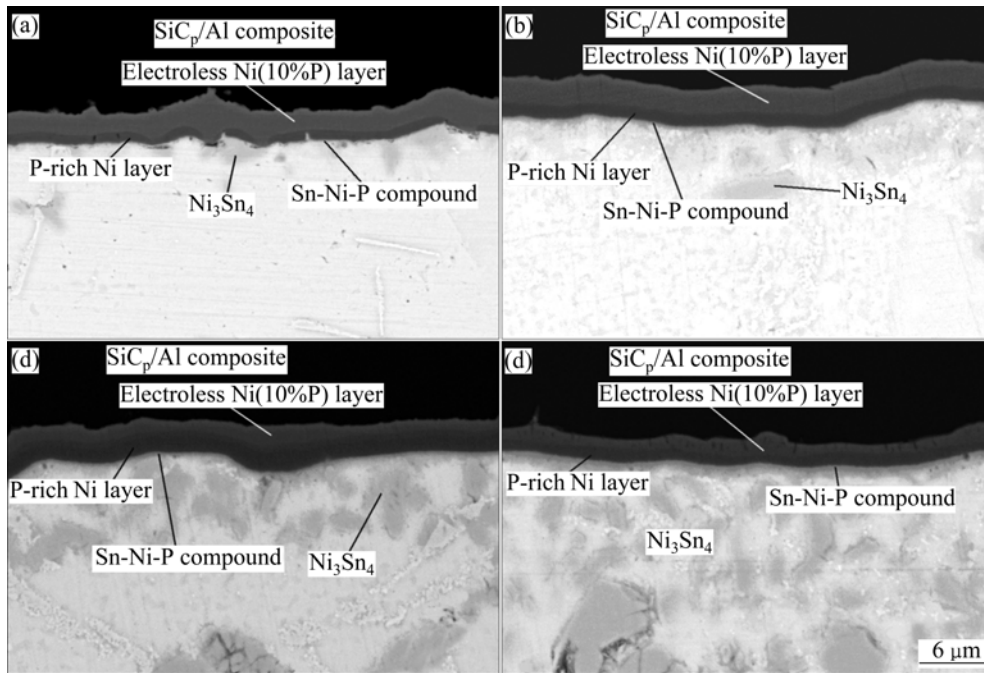


Fig.3 SEM images of SnAgNi/Ni(10 %P) solder joint aged at 150 °C for 50 h (a), 250 h (b), 500 h (c) and 1 000 h (d)

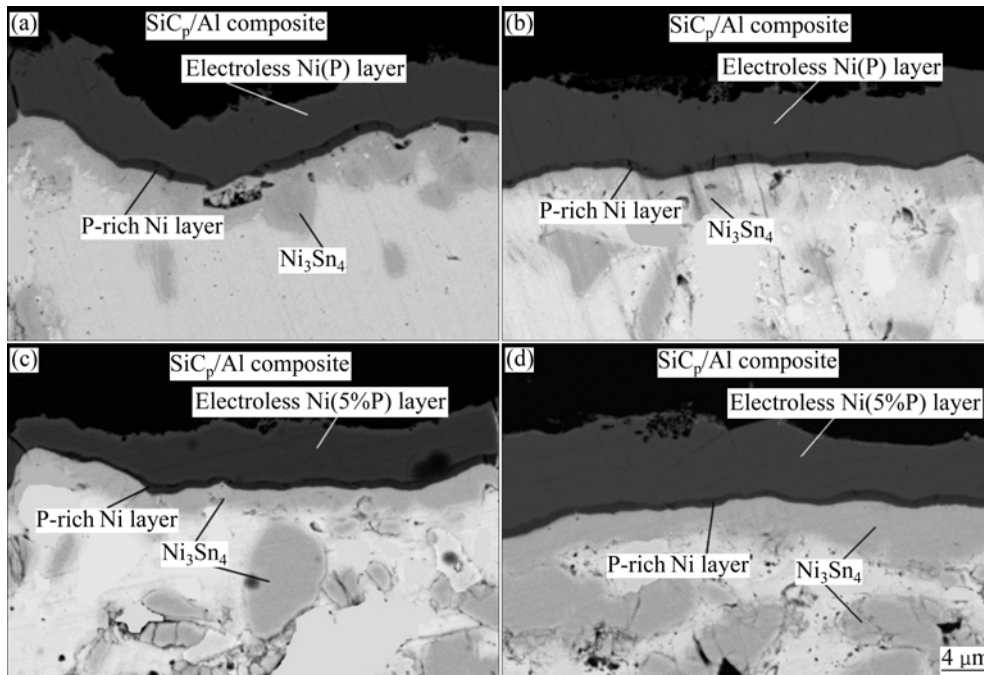


Fig.4 SEM images of SnAgNi/Ni(5%P) solder joint aged at 150 °C for 50 h (a), 250 h (b), 500 h (c) and 1 000 h (d)

growth of the intermetallic layer can be modeled by the parabolic growth kinetics[26]:

$$w=w_0+Kt^{1/2}$$

where w is the thickness of intermetallic layer at time t ; w_0 is the initial thickness of layer; K is the growth rate of the intermetallic layer; t is time. The calculated growth rate K for Ni_3Sn_4 in Ni(5%P) and Ni(10%P) solder joints

are 1.4×10^{-9} and 1.6×10^{-9} $\text{m/s}^{1/2}$, respectively. These results are very close to the values calculated by other studies[27]. Some studies have suggested that the lower growth exponent in experiments compared with that in the model is due to a transition of predominant transport mechanism from grain boundary diffusion to volume diffusion[28]. The $t^{1/2}$ dependence at 150 °C in this work suggests that volume diffusion is the rate controlling

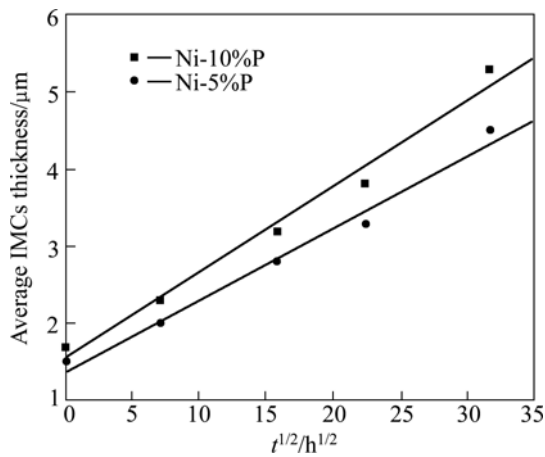


Fig.5 Relationship between average thickness of Ni_3Sn_4 layer and square root of aging time

mechanism. At higher temperatures, lattice diffusion becomes more significant than grain boundary diffusion.

3.3 Shear strength and fracture behavior

Owing to the presence of P, the reaction between Sn and Ni(P) is more complicated than that between Sn and pure Ni. Besides the existence of Ni layer, the formation of additional layers, such as the Ni-Sn-P, Ni_3P and Ni-P phases may influence the fracture behavior of the solder joint[27, 29]. The excessive growth of IMCs may be detrimental to the reliability of the solder joint because of the brittleness of the intermetallic layer, and the stress concentration generated from the volume change or

complete consumption of the solderable coating.

Shear strength of SnAgNi solder joint as a function of aging time is shown in Fig.6. Ni(5%P) layer yields the higher shear strength as compared with Ni(10%P) layer. Also it is clear from Figs.5 and 6 that with an increase in aging time, there is an increase in average thickness of IMCs and a decrease in shear strength. This implicates that with an increase in average thickness of IMCs, shear strength decreases.

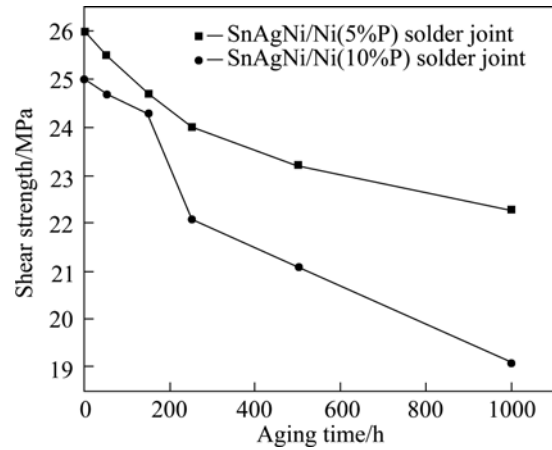


Fig.6 Relationship between shear strength of SnAgNi/Ni(P) solder joint and aging time

The fracture surface morphologies of Ni(5%P) solder joint aged at 150 °C and then subjected to shear test are shown in Fig.7. SEM images show that solder joint fails in a ductile mode before aging. It is observed

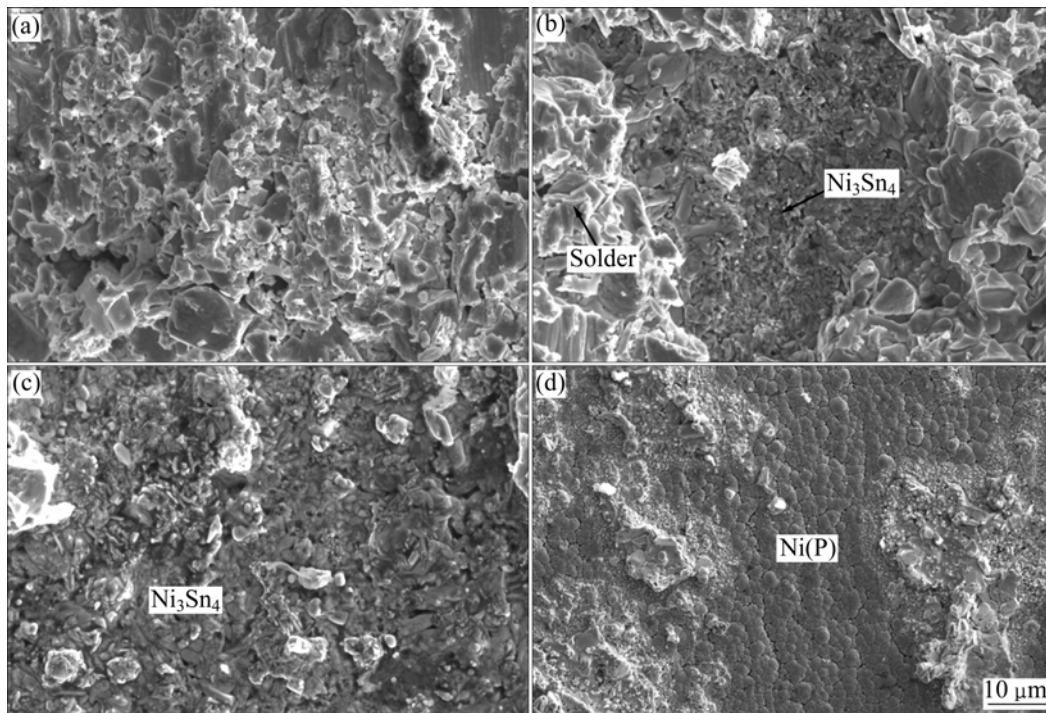


Fig.7 Fracture surface morphologies of SnAgNi/Ni(5%P) solder joint after aging for 0 h (a), 250 h (b), 500 h (c) and 1 000 h (d)

that fracture occurs at Ni_3Sn_4 /solder and Ni_3Sn_4 /Ni(P) interface after long term aging. The difference in coefficients of thermal expansion (CTE) values of Ni(P) layer, compact Ni_3Sn_4 IMC layer and solder generates thermal mismatch and stress at the interface of solder joints, which may initiate cracks at hard and brittle Ni_3Sn_4 IMC phase or may cause pre-existing cracks to grow. Thus, the growth of IMC layer and formation of cracks in these layers are the major sources of failure.

The cross-sectional morphologies of SnAgNi solder joint with Ni(10%P) layer subjected to a shear test are shown in Fig.8. It is obvious that the fracture occurs in the bulk solder and at the Ni_3Sn_4 /solder interface before aging. When aging at 150 °C for 50 h, the fracture occurs in the solder and at the solder/Ni-Sn-P interface. With further increase in aging time at the same temperature, the solder joint fails predominantly at solder/Ni-Sn-P interface and Ni(P)/ SiC_p /Al composites substrate interface. This failure results in a sharp fall in shear strength after 250 h aging. The continued reaction between Ni(P) layer and solder causes an excessive

depletion of Ni in remaining Ni(P) layer and this contributes to the generation of excessive amount of vacancies in Ni(P) layer especially near SiC_p /Al composites/Ni(P) interface due to directional diffusion of Ni towards the solder side. As a result, Kirkendall voids form after nucleation or condensation of vacancies. In other study, the formation of Kirkendall voids is also cited as a reason for the decrease of shear strength[14, 27]. The higher density of voids near SiC_p /Al composites/Ni(P) interface results in a poor adhesion between Ni(P) and SiC_p /Al composites.

From the observation above, three typical fracture patterns can be summarized as follows: 1) Ductile failure occurs inside the bulk solder. Before aging, the solder/IMC interface is usually quite rough and they penetrate each other, even stress concentration occurs at the interface, and the actual crack path along the interlocked interface requires more energy and greater applied load. 2) With further interface reaction, the solder/ Ni_3Sn_4 interface, solder/Ni(P) interface and solder/Ni-Sn-P interface become smoother due to the

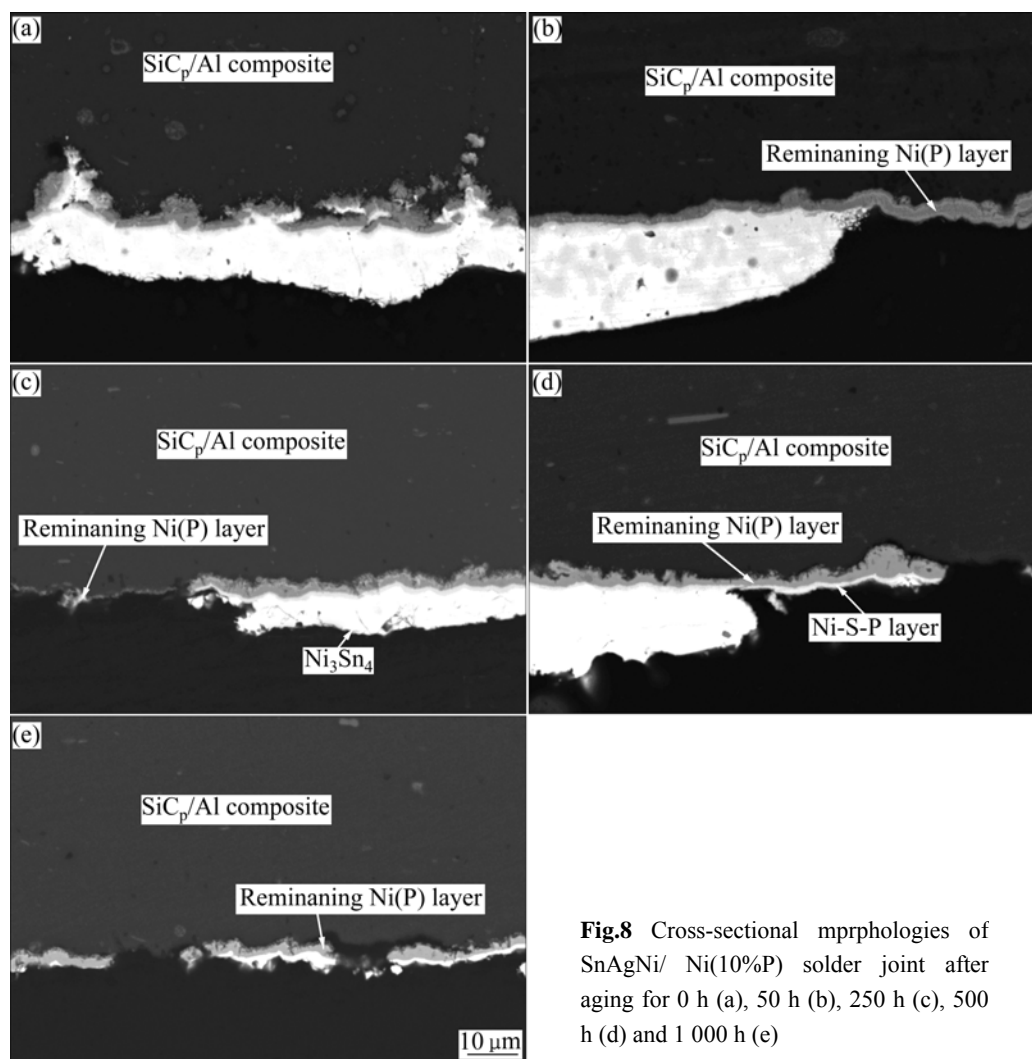


Fig.8 Cross-sectional morphologies of SnAgNi/ Ni(10%P) solder joint after aging for 0 h (a), 50 h (b), 250 h (c), 500 h (d) and 1 000 h (e)

tendency of reducing the interface area. As a result, the interface fracture strength is significantly reduced. Couple with the mismatch stress built up, the interface failure mode becomes dominant with longer aging time[30–31]. 3) Failure occurs inside the Ni_3Sn_4 layer or the interface between Ni coatings and substrate. The thickness of the Ni_3Sn_4 IMC increases after long time thermal aging. Fracture occurs in the IMC layer becomes possible because of its brittle nature. General trend is that with increasing the aging time, the fracture mode moves from solder failure to interfacial failure with a decreased strength.

4 Conclusions

1) $\text{Sn}_{2.5}\text{Ag}_{2.0}\text{Ni}$ alloy was utilized to solder SiC_p/Al composites substrates deposited with electroless Ni(5%P) and Ni(10%P) layers. Two kinds of microstructures are observed at the interface of SnAgNi solder and electroless Ni(P) layer due to the different contents of P.

2) The morphology of Ni_3Sn_4 IMCs in Ni(10%P) solder joint is found to be more needle-like and provides high speed diffusion channels for Ni to diffuse into solder, which leads to high growth rate of Ni_3Sn_4 . The diffusion of Ni into solder results in the Ni depletion in Ni(P) layer and ultimately leads to the formation of Kirkendall voids at the interface of Ni(P) layer and SiC_p/Al composites substrate. Solder reliability is observed to be degraded by the formation of Ni_2SnP , P-rich Ni layer and Kirkendall voids.

3) The compact Ni_3Sn_4 IMC layer in Ni(5%P) solder joint may prevent the diffusion of Ni element into solder, resulting in a low diffusion rate of Ni and a low growth rate of Ni_3Sn_4 layer. Meanwhile, the formation of Ni_2SnP significantly affects the reliability of solder joints, which is suppressed by the formation of stable Ni_3P layer in low P content Ni(5%P) layer. Thus, shear strength of Ni(5%P) solder joint is concluded to be higher than that of Ni(10%P) solder joint. In addition, growth of Ni_3Sn_4 IMC layer and formation of cracks are observed to be the major sources of failure for the solder joint with Ni(5%P).

References

- [1] CHUNG D D L, ZWEBEN C. Composites for electronic packaging and thermal management [C]// KELLY A, ZWEBEN C. Comprehensive Composite Materials, Amsterdam, 2003: 701–725.
- [2] CHUNG D D L. Materials for thermal conduction [J]. Appl Therm Eng, 2001, 21(16): 1593–1605.
- [3] ZWEBEN C. Advanced electronic packaging materials [J]. Adv Mater Process, 2005, 163(10): 33–37.
- [4] MOUSTAFA S F, HAMID Z A, ELHAY A M. Copper matrix SiC and Al_2O_3 particulate composites by powder metallurgy technique [J]. Mater Lett, 2002, 53(4/5): 244–249.
- [5] HU J, FEI W D. Investigation of the corroded surface of SiC_w/Al composite [J]. Appl Surf Sci, 2004, 239(1): 87–93.
- [6] GACSI Z, KOVACS J, PIECZONKA T, BUZA G. Investigation of sintered and laser surface remelted Al-SiC composites [J]. Surf Coat Tech, 2002, 151(3): 320–324.
- [7] FAN T X, SHI Z L, ZHANG D, WU R J. The interfacial reaction characteristics in SiC/Al composite above liquidus during remelting [J]. Mater Sci Eng A, 1998, 257(2): 281–286.
- [8] LI L B, AN M Z, WU G H. Model of electroless Ni deposition on SiC_p/Al composites and study of the interfacial interaction of coatings with substrate surface [J]. Appl Surf Sci, 2005, 252(4): 959–965.
- [9] YOON J W, JUNG S B. Investigation of interfacial reaction between Au-Sn solder and Kovar for hermetic sealing application [J]. Microelectron Eng, 2007, 84(11): 2634–2639.
- [10] ERIC C C, YAN S W, LEE R, HUANG X. Comparison of solder ball shear strength for various nickel platings on the band pads of a PBGA substrate [J]. Solder Surf Mt Tech, 2004, 16(2): 21–26.
- [11] SUN P, ANDERSSON C, WEI X C, CHENG Z N, SHANGGUAN D K, LIU J H. Study of interfacial reactions in Sn-3.5Ag-3.0Bi and Sn-8.0Zn-3.0Bi sandwich structure solder joint with Ni(P)/Cu metallization on Cu substrate [J]. J Alloy Compd, 2007, 437(1/2): 169–179.
- [12] SHARIF A, CHAN Y C. Liquid and solid state interfacial reactions of Sn-Ag-Cu and Sn-In-Ag-Cu solders with Ni-P under bump metallization [J]. Thin Solid Films, 2006, 504(1/2): 431–435.
- [13] AHAT S, SHENG M, LUO L. Effects of static thermal aging and thermal cycling on the microstructure and shear strength of $\text{Sn}_{95.5}\text{Ag}_{3.8}\text{Cu}_{0.7}$ solder joints [J]. J Mater Res, 2001, 16(10): 2914–2921.
- [14] AHAT S, DU L G, SHENG M, LUO L, KEMPE W, FREYTAG J. Effect of aging on the microstructure and shear strength of SnPbAg/Ni-P/Cu and SnAg/Ni-P/Cu solder joints [J]. J Electron Mater, 2000, 29(9): 1105–1109.
- [15] ALAM M O, CHAN Y C, HUNG K C. Reliability study of the electroless Ni-P layer against solder alloy [J]. Microelectron Reliab, 2002, 42(7): 1065–1073.
- [16] LIN Y C, SHIH T Y, TIEN S K, DUH J G. Suppressing Ni-Sn-P growth in SnAgCu/Ni-P solder joints [J]. Scripta Mater, 2007, 56(1): 49–52.
- [17] LIN Y C, DUH J G. Phase transformation of the phosphorus-rich layer in SnAgCu/Ni-P solder joints [J]. Scripta Mater, 2006, 54(9): 1661–1665.
- [18] KANG H B, BAE J H, LEE J W, PARK M H, LEE Y C, YOON J W, JUNG S B, YANG C W. Control of interfacial reaction layers formed in Sn-3.5Ag-0.7Cu/electroless Ni-P solder joints [J]. Scripta Mater, 2009, 60(4): 257–260.
- [19] SOHN Y C, YU J, KANG S K, SHIH D Y, LEE T Y. Spalling of intermetallic compounds during the reaction between lead-free solders and electroless Ni-P metallization [J]. J Mater Res, 2004, 19(8): 2428–2436.
- [20] ZENG K, TU K N. Six cases of reliability study of Pb-free solder joints in electronic packaging technology [J]. Mater Sci Eng R, 2002, 38(2): 55–105.
- [21] KIM S W, YOON J W, JUNG S B. Interfacial reactions and shear strengths between Sn-Ag-based Pb-free solder balls and Au/EN/Cu

- metallization [J]. *J Electron Mater*, 2004, 33(10): 1182–1189.
- [22] KIM H K, TU K N, TOTTA P A. Ripening-assisted asymmetric spalling of Cu-Sn compound spheroids in solder joints on Si wafers [J]. *Appl Phys Lett*, 1996, 68(16): 2204–2206.
- [23] LIU P L, SHANG J K. Thermal stability of electroless-nickel/solder interface: Part B. Interfacial fatigue resistance [J]. *Metallurgical and Materials Transactions*, 2000, 31A: 2867–2875.
- [24] STAIA M H, PUCHI E S, GASTRO G, RAMIREZ F O, LEWIS D B. Effect of thermal history on the microhardness of electroless Ni-P [J]. *Thin solid Films*, 1999, 355/356: 472–479.
- [25] JANG J W, KIM P G, TU K N. Solder reaction-assisted crystallization of electroless Ni-P under bump metallization in low cost flip chip technology [J]. *J Appl Phys*, 1999, 85(12): 8456–8463.
- [26] WU Y, SEES J A, POURAGHABAGHER C, FOSTER L A, MARSHALL J L, JACOBS E G, PINIZZOTTO R F. The formation and growth of intermetallics in composite solder [J]. *J Electron Mater*, 1993, 22(7): 769–777.
- [27] CHEN Z, HE M, KUMAR A, QI G J. Effect of interfacial reaction on the tensile strength of Sn-3.5Ag/Ni-P and Sn-37Pb/Ni-P solder joints [J]. *J Electron Mater*, 2007, 36(1): 17–25.
- [28] MATT S, RAYMOND A. Theory for intermetallic phase growth between Cu and liquid Sn-Pb solder based on grain boundary diffusion control [J]. *J Electron Mater*, 1998, 27(11): 1167–1176.
- [29] CHEN Z, HE M, QI G J. Morphology and kinetic study of the interfacial reaction between the Sn-3.5Ag solder and electroless Ni-P metallization [J]. *J Electron Mater*, 2004, 33(12): 1465–1472.
- [30] LEE H T, CHEN M H. Influence of intermetallic compounds on the adhesive strength of solder joints [J]. *Mater Sci Eng A*, 2002, 333(1/2): 24–34.
- [31] FREAR D R, VIANCO P T. Intermetallic growth and mechanical behavior of low and high melting temperature solder alloys [J]. *Metall Mater Trans A*, 1994, 25A(7): 1509–1523.

(Edited by FANG Jing-hua)